

RESEARCH

Open Access



Dyslipidemia and aging: the non-linear association between atherogenic index of plasma (AIP) and aging acceleration

QianKun Yang^{1*†}, XianJie Zhu^{1,2†}, Li Zhang^{3,4†} and Fei Luo^{1*}

Abstract

Background Dyslipidemia has been proved to play a pivotal role in biological aging. Atherogenic Index of Plasma (AIP), derived from serum triglyceride (TG) and high-density lipoprotein cholesterol (HDL-C), is an effective biomarker of dyslipidemia. However, whether AIP can be used as an indicator of biological aging remains unclear. This study aims to investigate the relationship between AIP and biological aging in the US adult population.

Methods 4,471 American adults with age over 20 years from the National Health and Nutrition Examination Survey (NHANES) database were included in this study. Biological aging was assessed by phenotypic age acceleration (PhenoAgeAccel). Multivariable linear regression models, subgroup analyses and interaction tests were employed to explore the association between AIP and PhenoAgeAccel. Furthermore, adjusted restricted cubic spline (RCS) analyses were employed to assess potential nonlinear relationships, while mediation analysis was utilized to identify the mediating effects of homeostatic model assessment of insulin resistance (HOMA-IR). Besides, network pharmacology was performed to determine the potential mechanisms underlying dyslipidemia-related aging acceleration.

Results A total of 4,471 participants were included in this study, the median chronological age, PhenoAge and PhenoAgeAccel for the overall population were 49 (35–64) years, 42.85 (27.30–59.68) years, and –6.92 (–10.52 to –2.46) years, respectively. In the fully adjusted model, one unit increase of AIP was correlated with 1.820-year increase in PhenoAgeAccel ($\beta = 1.820$, 95% CI: 1.085–2.556), which was more pronounced among individuals being female, diabetic and hypertensive. Furthermore, RCS analysis revealed a nonlinear relationship between AIP and PhenoAgeAccel, with an inflection point identified at –0.043 for AIP via threshold and saturation effect analysis. AIP demonstrated a positive correlation with PhenoAgeAccel both before ($\beta = 6.550$, 95% CI: 5.070–8.030) and after ($\beta = 3.898$, 95% CI: 2.474–5.322) this inflection point. Additionally, HOMA-IR was found to mediate 39.21% of the association between AIP and PhenoAgeAccel. Finally, network pharmacology analysis identified INS, APOE, APOB, IL6, IL10, PPARG, MTOR, ACE, PPARGC1A, and SERPINE1 as core targets in biological aging, which were functionally linked to key signaling pathways like AMPK, apelin, JAK-STAT, FoxO, etc.

[†]QianKun Yang, XianJie Zhu, Li Zhang contribute equally to this work.

*Correspondence:

QianKun Yang
yqk1991@tmmu.edu.cn
Fei Luo
luofei@tmmu.edu.cn

Full list of author information is available at the end of the article



© The Author(s) 2025. **Open Access** This article is licensed under a Creative Commons Attribution-NonCommercial-NoDerivatives 4.0 International License, which permits any non-commercial use, sharing, distribution and reproduction in any medium or format, as long as you give appropriate credit to the original author(s) and the source, provide a link to the Creative Commons licence, and indicate if you modified the licensed material. You do not have permission under this licence to share adapted material derived from this article or parts of it. The images or other third party material in this article are included in the article's Creative Commons licence, unless indicated otherwise in a credit line to the material. If material is not included in the article's Creative Commons licence and your intended use is not permitted by statutory regulation or exceeds the permitted use, you will need to obtain permission directly from the copyright holder. To view a copy of this licence, visit <http://creativecommons.org/licenses/by-nc-nd/4.0/>.

Conclusions An elevated AIP was notably and positively correlated with accelerated aging, suggesting that AIP may serve as an effective predictor to evaluate accelerated aging.

Graphical Abstract

Dyslipidemia and Aging: The non-linear association between Atherogenic Index of Plasma (AIP) and Aging Acceleration

Study design:

- Cross-sectional study based on Nhanes database
- Exposure: Atherogenic Index of Plasma (AIP)
- Outcome: phenotypic age acceleration (PhenoAgeAccel)
- Covariates: age, gender, race, education, etc.
- Mediator: HOMA-IR

Results:

1. Multivariable linear regression analyses

Exposure	Fully Adjusted model β (95% CI) P-value
AIP	1.820 (1.085, 2.556) <0.00001
AIP quartile	
Q1	0
Q2	1.100 (0.537, 1.663) 0.00013
Q3	1.178 (0.597, 1.759) 0.00007
Q4	1.582 (0.970, 2.194) <0.00001
P for trend	<0.00001

2. Subgroup analyses

3. Mediating effect analyses

ACME=0.3011, P<0.0001
 Proportion of mediation: 33.21%
 ADE=0.4669, P=0.0040

4. Adjusted restricted cubic spline (RCS) analyses

5. Stratified RCS analyses

6. Network pharmacology

Conclusion: An elevated AIP was notably and positively correlated with accelerated aging, with such association being more pronounced in female, diabetic and hypertensive individuals.

Keywords PhenoAgeAccel, Atherogenic index of plasma, Accelerated aging, Dyslipidemia

Introduction

Accelerated demographic aging poses a pressing challenge to public health systems globally, given its established role as a primary etiological contributor to the pathogenesis of prevalent noncommunicable conditions [1, 2]. Therefore, preventive strategies and interventions aimed at facilitating healthy aging are critical. Although everyone ages, the aging rate remains heterogeneous, and such heterogeneity in aging pace is reflected by the different susceptibility to death and disease. Identifying biological aging patterns in individuals of the same age, particularly in early life, supports targeted prevention by pinpointing high-risk groups for age-related diseases. However, how to measure aging remains a critical issue. Additionally, for clinical application, these assessments should be easy to operate on existing platforms, better at risk stratification than traditional metrics, and able to

identify preclinical risk markers before disease onset or functional decline.

A validated approach for assessing biological age acceleration involves benchmarking an individual's functional biomarkers and physiological parameters against population-level normative data in the general population stratified by chronological age. Numerous aging measures have been established using molecular markers or indicators, with the most prominent and representative indicators being the epigenetic clocks (also named DNA methylation age) [3] and leukocyte telomere length [4]. However, these cellular-level indicators, predominantly derived from single-tissue or blood-based measurements, demonstrate greater utility in evaluating organ-specific aging processes, while exhibiting limited effectiveness in assessing the efficacy of geroprotective interventions or broader health-span related outcomes

[5]. Actually, several studies have revealed that while these indicators are phenomenal age predictors, they exhibit weak to moderate associations with aging outcomes when excluded what can be explained by chronological age [1, 5–8]. For example, the study conducted by Marioni et al. [6] suggested that lower physical and mental fitness markers are correlated with epigenetic age acceleration, but the latter does not predict short-term declines in these fitness measures. In contrast, aging measures derived from clinically observable data or characteristics, such as Phenotypic Age, integrate multisystem physiological information across the organism and tend to be more robust in predicting aging outcomes [5, 9, 10]. Such difference in prediction between molecular and clinical measures lie in that the former only draw information from limited dimensions of the multifactorial aging process, whereas the latter capture multiple aspects of diverse aging hallmarks occurred across cellular and intracellular levels [1, 5]. Although composite scores from traditional clinical chemistry measures don't offer mechanistic insights, their superior performance, affordability, and practicality compared to current molecular measures make them more suitable for assessing anti-aging effects at the whole level and identifying high-risk groups for death and disease [5].

Phenotypic Age (PhenoAge) is one of the existing clinical measures which integrate multiple clinical chemistry biomarkers based on parametrization from a Gompertz mortality model [11]. Given that the heterogeneity of aging rates between persons, chronological time is actually an inaccurate proxy to establish an aging measure [12]. Therefore, unlike previously established aging measures that were generated based on the associations between their constituent variables and chronological age, PhenoAge was formulated and optimized to differentiate mortality risk among individuals with the same chronological age by using various multi-system clinical chemistry biomarkers [1]. Generally, a person's PhenoAge represents the age in the general population that aligns with that person's mortality risk. PhenoAge acceleration (PhenoAgeAccel) represents the deviation between PhenoAge and chronological age. A person with a positive PhenoAgeAccel signifies that he/she has a higher average mortality risk than what he/she should have in that chronological age. Currently, PhenoAge, serving as a predictive or outcome indicator, has been widely applied in various aspects, including: (1) predicting risks of mortality, disease onset, functional decline in patients with diverse diseases [13–15]; (2) assessing the effects of environmental factors (e.g., tobacco exposure [16]), behavioral factors (e.g., omega-3 fatty acid intake, vitamin D supplementation, physical exercise [17, 18]), and anti-aging interventions (e.g., metformin [19]) on aging acceleration. Briefly, PhenoAge is an indicator

closely linked to an individual's risks of adverse health outcomes and capable of reflecting the overall degree of an individual's aging.

Dyslipidemia is a significant modifiable risk factor tightly associated with biological aging and aging-related diseases [20–22], with its typical characteristics being elevated levels of total cholesterol (TC), triglycerides (TG), and low-density lipoprotein cholesterol (LDL-C), and reduced levels of high-density lipoprotein cholesterol (HDL-C) [22]. Several composite indicators were established based on these variables and proved to be significantly associated with the adverse outcomes of various diseases, including the TG/LDL-C ratio [23], non-HDL-C to HDL-C ratio (NHHR) [24], remnant cholesterol (RC) [25], atherogenic Index of plasma (AIP) [26], etc.. Notably, AIP, calculated as $\log_{10}(\text{TG}/\text{HDL})$, has been established as a superior predictor among dyslipidemia-related indicators, which exhibits robust associations not only with dyslipidemia itself but also with a spectrum of cardiometabolic disorders, including cardiovascular diseases, diabetes, metabolic syndrome, and hypertension [27–30]. This can be illustrated by the following facts. Firstly, in contrast to other dyslipidemia indicators, AIP integrates two atherogenic lipid parameters—triglycerides (TG) and high-density lipoprotein cholesterol (HDL-C)—via a logarithmic transformation of their ratio ($\log_{10}(\text{TG}/\text{HDL-C})$). This nonlinear transformation amplifies sensitivity to dynamic metabolic abnormalities [31]. Moreover, AIP shows a pronounced correlation with the particle diameter of small dense LDL (sdLDL), a key driver of atherosclerosis [32]. This enables AIP to mirror the underlying pathogenic mechanisms, which is a crucial edge over traditional metrics mentioned above. Additionally, AIP demonstrates consistent predictive validity on health outcomes (e.g., cardiovascular outcomes [31, 33–35], diabetes mellitus [28, 36, 37]) across diverse ethnicities, age groups, and clinical conditions. Finally, except for dyslipidemia, AIP outperforms other indicators in identifying metabolic disorders such as insulin resistance [28], metabolic syndrome [27], diabetes mellitus [37], and so on. AIP was proved to show an inverse L-shaped and a J-shaped association with homeostasis model assessment of insulin resistance (HOMA-IR) and diabetes mellitus [28], respectively. Interestingly, HOMA-IR has been reported to positively and non-linearly correlate with biological age and advanced aging [38]. Consequently, AIP possesses the potential to serve as potent biomarker not only for glycometabolic disorders but also for the process of aging. Briefly, given the crucial role of dyslipidemia in the aging process and the unique advantages of AIP in mirroring dyslipidemia, it is reasonable to speculate that a strong link might exist between AIP and aging acceleration. Nonetheless, the clinical and statistical relationships between AIP and

aging, along with relevant mediating factors, and the core genes or key mechanisms underlying dyslipidemia-related accelerated biological aging, all await further clarification.

Therefore, we aim to explore the potential link between AIP and accelerated aging by using the NHANES database. Meanwhile, network pharmacology was employed to explore the core genes or key mechanisms underlying such aging acceleration. Our findings are anticipated to provide valuable insights concerning biological aging, which could potentially help to improve the management and prevention of the aging process and age-related diseases.

Methods

Study design and data source

This cross-sectional study utilized data from the National Health and Nutrition Examination Survey (NHANES), which is a nationally representative dataset curated by the Centers for Disease Control and Prevention (CDC). NHANES merges interviews, physical examinations, laboratory assessments and questionnaire data to furnish

comprehensive health and nutritional profiles of the U.S. populace. To obtain a representative sample of the U.S. population, a stratified, multistage, and probabilistic sampling methodology was implemented [39]. This method guarantees that every member of the target population has a well-defined, non-zero probability of being selected, and it employs randomization to eliminate selection bias, thus ensuring the sample representativeness and valid generalizations [40, 41]. All NHANES protocols received approval from the Research Ethics Review Board of the National Center for Health Statistics, and written informed consent was obtained from all survey participants. Comprehensive information regarding the NHANES study and its associated data can be found on the official website at <https://www.cdc.gov/nchs/nhanes>.

Study population

This study included participants from 2007 to 2010, as C-reactive protein data utilized for calculating PhenoAge has not been available since 2011 [39].

Participants aged 20 years and above who had complete data on PhenoAge, AIP, and other key covariates

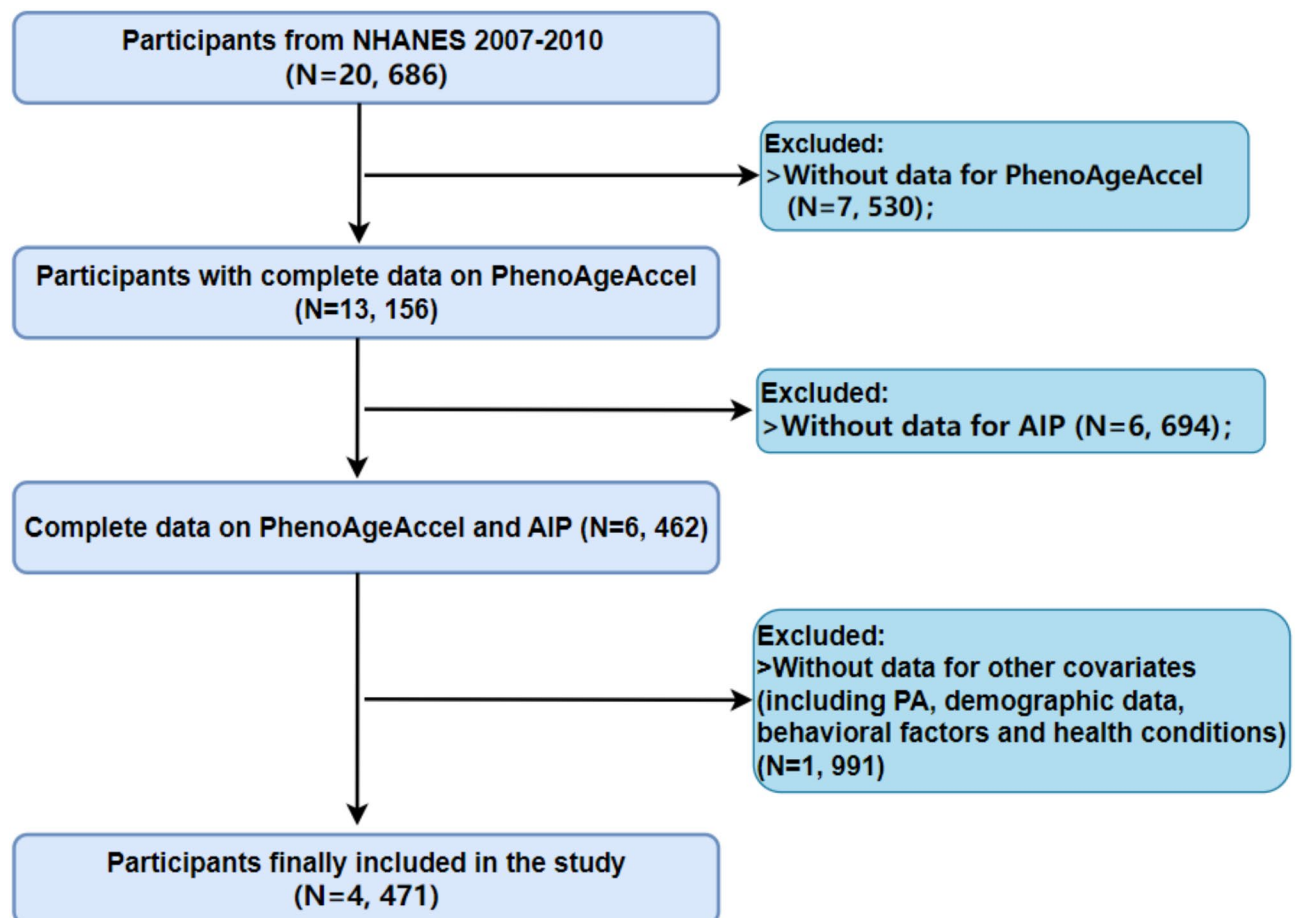


Fig. 1 Flow chart of participants selection

were included in the analysis. We excluded those with incomplete PhenoAge data (N=7,530) and individuals lacking AIP data (N=6,694). Furthermore, participants without sufficient information on physical activity, demographic details, body mass index, behavioral factors, and health conditions were also removed from the analysis. As a result, a total of 4,471 individuals were included in the final analysis. A flowchart detailing the selection process of participants was presented in Fig. 1.

Assessment of atherogenic index of plasma (AIP) and HOMA-IR

The atherogenic index of plasma (AIP) is calculated using the formula as previously described [42, 43]: $AIP = \log[TG(\text{mmol/L})/HDL-C(\text{mmol/L})]$, where TG represents triglycerides and HDL-C stands for high-density lipoprotein cholesterol. The homeostatic model assessment of insulin resistance (HOMA-IR) can be determined using the formula: $HOMA-IR = [\text{fasting serum insulin } (\mu\text{U/mL}) \times \text{FPG (mg/dL)}] / 405$, where FPG denotes the concentration of fasting plasma glucose, as previously detailed [44].

Assessment of PhenoAgeAccel

Details regarding the definition of PhenoAge and PhenoAgeAccel are provided in the supplementary materials (Supplementary Method 1). Briefly, based on the definition of PhenoAge established by Levine et al. [11], the PhenoAge was calculated using ten variables associated with aging, including chronological age, albumin, creatinine, glucose, C-reactive protein, lymphocyte percentage, mean cell volume, red blood cell distribution width, alkaline phosphatase, and white blood cell count (Supplementary Table 1). The comprehensive protocols for sample collection, preservation, processing, and analysis required to obtain these data have been detailedly reported elsewhere [17, 39].

PhenoAge Acceleration (PhenoAgeAccel) is defined as the residual from a linear model in which Phenotypic Age is regressed on chronological age [1, 17, 39]. Consequently, PhenoAgeAccel denotes the phenotypic age with the consideration of chronological age. In other words, it reflects whether, in terms of physiology, an individual seems older (indicated by a positive value) or younger (indicated by a negative value) than what would be anticipated according to their actual age. In this study, individuals with positive PhenoAgeAccel values were classified as the aging-acceleration group, while those with non-positive values were classified as the non-aging-acceleration group.

Covariates

The covariates included in the current study were physical activity (PA), demographic details (including age,

gender, race, education level, poverty income ratio and marital status), BMI, behavioral factors (smoking, drinking), and health conditions (including diabetes, cardiovascular disease, and hypertension). Among these variables, race/ethnicity was classified as Mexican American, non-Hispanic White, non-Hispanic Black, other Hispanic, and other. Education levels were divided into three levels as previously described [45–47], including less than high school, high school or equivalent, and some college or above. Marital status was grouped into three categories as referred to previous studies [45–47], including married, never married and others. Individuals were diagnosed as having diabetes with any of the following criteria [48]: (1) hemoglobin A1C level of 6.5% or a fasting plasma glucose concentration of ≥ 126 mg/dL; (2) answered “yes” to the question of “Doctor told you have diabetes? or Taking insulin now?”; (3) with fasting glucose ≥ 7.00 mmol/L; (4) with the two-hour oral glucose tolerance test (OGTT) ≥ 11.10 mmol/L; (5) with random blood glucose ≥ 11.10 mmol/L; (6) taking diabetic medication or insulin for treatment now. Hypertension can be identified among those who meet one or more of the following conditions [49]: (1) individuals who responded “yes” to the question of “Has a doctor or any other health professional ever told you that you had hypertension?”; (2) with average systolic blood pressure (SBP) was ≥ 130 mmHg or the average diastolic blood pressure (DBP) ≥ 80 mmHg; (3) taking any anti-hypertensive drug for treatment currently. The five principal CVD events, including congestive heart failure (CHF), coronary heart disease (CHD), angina, cardiac arrest, and stroke were utilized to define cardiovascular disease (CVD) [48]. Individuals who answered “yes” to the question of “Have you ever been told by a physician that you had CHD/CHF/angina/a heart attack or a stroke?” were diagnosed as having CVD. Physical activity (PA) was evaluated based on the Global Physical Activity Questionnaire (GPAQ), which included the frequency and duration of vigorous and moderate of activities. The assessment of PA encompassed both the frequency (number of sessions per week) and the duration (length of time each session) of exercise. Previously studies have revealed that one minute of vigorous PA is equivalent to two minutes of moderate-intensity PA [45–47]. Given this, the weekly total PA can be calculated by the following formula: $2 \times \text{vigorous PA} + \text{moderate PA}$.

Alcohol consumption status was classified into four categories [47]: never drinker, formal drinker, current drinker, and missing. Specifically, individuals who had never consumed 12 alcoholic beverages were classified as never-drinkers. Those who had consumed 12 drinks but had stopped drinking were designated as former drinkers. In contrast, individuals who had consumed at least 12 drinks and had at least one drink in the past

12 months were identified as current drinkers. Participants with incomplete drinking data were categorized as missing data. Smoking status was classified into three categories—never smokers, former smokers, and current smokers—based on self-reported questionnaire data as previously detailed [47]. Individuals who had never smoked 100 cigarettes in their lifetime were designated as never smokers. Those who had smoked 100 cigarettes but had subsequently ceased were categorized as former smokers, while individuals who had smoked 100 cigarettes and continued to smoke were identified as current smokers.

Network pharmacological analysis

In order to further explore the potential targets and mechanisms of cholesterol metabolism, triglyceride metabolism and insulin resistance in relation to biological aging, we conducted the network pharmacological analysis. Firstly, the genes responsible for the above-mentioned four biological processes were obtained from the GeneCards database (<https://www.genecards.org/>) and Online Mendelian Inheritance in Man (OMIM) database using the key words of “cholesterol metabolism”, “insulin resistance”, “triglyceride metabolism”, and “biological aging”, respectively. Then, the intersection targets among the four biological processes were identified using Venny 2.1 (<https://bioinfogp.cnb.csic.es/tools/venny/>). Furthermore, the protein–protein interactions (PPIs) of the overlapping genes were analyzed in the STRING database (<https://string-db.org/>), and the PPI network was established by Cytoscape (Version 3.8.2) software. The determination of the top 10 core targets was based on the comprehensive judgement of betweenness, closeness and degree of the PPI nodes [50]. Finally, the intersection targets were subsequently uploaded to the Database for Annotation, Visualization, and Integrated Discovery (DAVID, <http://david.abcc.ncifcrf.gov/>) to conduct analyses for the Kyoto Encyclopedia of Genes and Genomes (KEGG) and Gene Ontology (GO). GO terms and KEGG pathways were deemed significant if they had a P-value less than 0.05.

Statistical analysis

The appropriate NHANES sampling weights, as well as the intricate multistage cluster survey design were taken into account in all statistical analyses. NHANES sampling weights are created to handle the complex survey design (oversampling), non-response and post-stratification adjustment to ensure representativeness of the U.S. civilian noninstitutionalized population, with each weight reflecting the theoretical population count represented by the participant [51]. The baseline characteristics of the participants were presented based on the quartiles of AIP, and continuous variables were described as median

and interquartile ranges (IQR) due to their non-normal distributions while categorical variables were exhibited as frequencies and percentages. The differences in characteristics across AIP categories were compared using Rao-Scott chi-squared test or Kruskal–Wallis test.

Multivariable linear regression models were established to assess the association between AIP and PhenoAgeAccel, among which AIP was analyzed as both a categorical variable (quartiles) and continuous variable (the β value being calculated for each unit increase). Three models were established: Model 1 was adjusted for no covariate; Model 2 was adjusted for age, gender, race, education, marital status, and PIR; Model 3 was further adjusted for BMI, diabetes, hypertension, CVD, smoking, alcohol consumption, and PA based on Model 2. Moreover, to explore the dose–response relationship between AIP and PhenoAgeAccel, restricted cubic splines (RCSs) based on multivariable linear regression models was conducted. As previously described [38], the number of nodes was initially set between 3 and 5, and further determined based on the lowest AIC value for each setting. If a non-linear relationship between AIP and PhenoAgeAccel was identified, the “segmented” package was used to determine the inflection point, relying on the results of likelihood-ratio test and the bootstrap resampling method [24]. Also, associations between AIP and PhenoAgeAccel on both sides of the breakpoint were assessed using segmented multivariable linear regression model.

To identify the robustness and stability of AIP-PhenoAgeAccel association, subgroup analyses and interaction tests were also conducted based on variables of gender, age, BMI, education, marital status, PIR, diabetes, hypertension, CVD, smoking and drinking. If the interaction test yielded significant results, subsequent stratified RCS analyses were conducted to examine potential variations in the AIP-PhenoAgeAccel association across subgroups stratified by the identified effect-modifying variable. Additionally, the R package of ‘mediation’ was performed to investigate the mediation effects of HOMA-IR on AIP-PhenoAgeAccel association after adjusting covariates included in model 3 as previously described [52]. Briefly, the mediation analysis employed two sequential models: a mediator model assessing the association between AIP (exposure) and HOMA-IR (mediator), and an outcome model simultaneously incorporating AIP and HOMA-IR to quantify their effects on PhenoAgeAccel (outcome). The mediation percentage is calculated to quantify the magnitude of the mediation effect, which is defined as the ratio of the indirect effect to the total effect. Bootstrap resampling with 1000 iterations was utilized to test the significance of mediation effect [53].

All statistical analyses were performed using R software (version 4.4.2, <https://cran.r-project.org/bin/windows/base/>), with a significance threshold of $P < 0.05$ (two-tailed).

Table 1 Baseline characteristics of the study participants

Characteristic	Overall	AIP				P value
		Q1	Q2	Q3	Q4	
Age (years)	49.00 (35.00–64.00)	45.00 (32.00–61.00)	50.00 (34.00–65.25)	51.00 (35.00–66.00)	51.00 (38.00–64.00)	< 0.001
PIR	2.06 (1.10–4.08)	2.35 (1.22–4.31)	2.09 (1.09–4.14)	2.09 (1.16–3.98)	1.71 (0.97–3.49)	< 0.001
BMI (kg/m ²)	27.84 (24.26–32.21)	24.95 (21.89–28.72)	27.27 (23.97–31.19)	29.00 (25.51–32.99)	29.94 (26.88–34.23)	< 0.001
PA (minutes)	174.28 (374.21)	219.05 (424.19)	164.58 (341.21)	178.00 (401.10)	135.53 (315.64)	< 0.001
PhenoAge (years)	42.85 (27.30–59.68)	36.43 (23.10–53.56)	43.27 (26.85–60.26)	44.91 (28.57–61.21)	46.49 (32.48–61.75)	< 0.001
PhenoAgeAccel (years)	−6.92 (−10.52 to −2.46)	−9.45 (−12.10 to −4.83)	−7.12 (−10.27 to −2.66)	−6.27 (−10.08 to −2.00)	−5.70 (−8.93 to −0.88)	< 0.001
Gender (%)						< 0.001
Male	2137 (47.80%)	371 (33.24%)	514 (46.06%)	579 (51.65%)	673 (60.20%)	
Female	2334 (52.20%)	745 (66.76%)	602 (53.94%)	542 (48.35%)	445 (39.80%)	
Race (%)						< 0.001
Mexican American	798 (17.85%)	124 (11.11%)	182 (16.31%)	241 (21.50%)	251 (22.45%)	
Other hispanic	452 (10.11%)	105 (9.41%)	101 (9.05%)	111 (9.90%)	135 (12.08%)	
Non-hispanic white	2213 (49.50%)	513 (45.97%)	576 (51.61%)	535 (47.73%)	589 (52.68%)	
Non-hispanic black	800 (17.89%)	321 (28.76%)	199 (17.83%)	182 (16.24%)	98 (8.77%)	
Other races	208 (4.65%)	53 (4.75%)	58 (5.20%)	52 (4.64%)	45 (4.03%)	
Education (%)						< 0.001
Less than high school	1286 (28.76%)	238 (21.33%)	301 (26.97%)	328 (29.26%)	419 (37.48%)	
High school or equivalent	1043 (23.33%)	221 (19.80%)	267 (23.92%)	282 (25.16%)	273 (24.42%)	
Some college or above	2142 (47.91%)	657 (58.87%)	548 (49.10%)	511 (45.58%)	426 (38.10%)	
Marital status (%)						< 0.001
Married	2365 (52.90%)	526 (47.13%)	596 (53.41%)	623 (55.58%)	620 (55.46%)	
Never married	728 (16.28%)	241 (21.59%)	174 (15.59%)	164 (14.63%)	149 (13.33%)	
Others	1378 (30.82%)	349 (31.27%)	346 (31.00%)	334 (29.79%)	349 (31.22%)	
Diabetes (%)						< 0.001
Yes	501 (11.21%)	75 (6.72%)	102 (9.14%)	144 (12.85%)	180 (16.10%)	
No	3970 (88.79%)	1041 (93.28%)	1014 (90.86%)	977 (87.15%)	938 (83.90%)	
Hypertension (%)						< 0.001
Yes	1581 (35.36%)	295 (26.43%)	379 (33.96%)	430 (38.36%)	477 (42.67%)	
No	2890 (64.64%)	821 (73.57%)	737 (66.04%)	691 (61.64%)	641 (57.33%)	
CVD (%)						< 0.001
No	3987 (89.17%)	1032 (92.47%)	996 (89.25%)	1008 (89.92%)	951 (85.06%)	
Yes	484 (10.83%)	84 (7.53%)	120 (10.75%)	113 (10.08%)	167 (14.94%)	
Smoking (%)						< 0.001
Never smoker	2402 (53.72%)	706 (63.26%)	618 (55.38%)	570 (50.85%)	508 (45.44%)	
Former smoker	1136 (25.41%)	223 (19.98%)	277 (24.82%)	313 (27.92%)	323 (28.89%)	
Current smoker	933 (20.87%)	187 (16.76%)	221 (19.80%)	238 (21.23%)	287 (25.67%)	
Alcohol consumption (%)						< 0.001
Never drinker	536 (11.99%)	142 (12.72%)	142 (12.72%)	128 (11.42%)	124 (11.09%)	
Former drinker	789 (17.65%)	144 (12.90%)	174 (15.59%)	216 (19.27%)	255 (22.81%)	
Current drinker	2840 (63.52%)	734 (65.77%)	726 (65.05%)	702 (62.62%)	678 (60.64%)	
Missing	306 (6.84%)	96 (8.60%)	74 (6.63%)	75 (6.69%)	61 (5.46%)	
Aging Acceleration (%)						< 0.001
No	3758 (84.05%)	1008 (90.32%)	956 (85.66%)	927 (82.69%)	867 (77.55%)	
Yes	713 (15.95%)	108 (9.68%)	160 (14.34%)	194 (17.31%)	251 (22.45%)	

AIP, atherogenic index of plasma; CVD, cardiovascular disease; BMI, body mass index; PIR, ratio of family income to poverty; Q, quartile; PA, physical activity; PhenoAge, phenotypic age; PhenoAgeAccel, phenotypic age acceleration

Variables of age, PIR, BMI, AIP, PhenoAge and PhenoAgeAccel were presented as Median (Q1-Q3) due to their non-normal distribution characteristics.

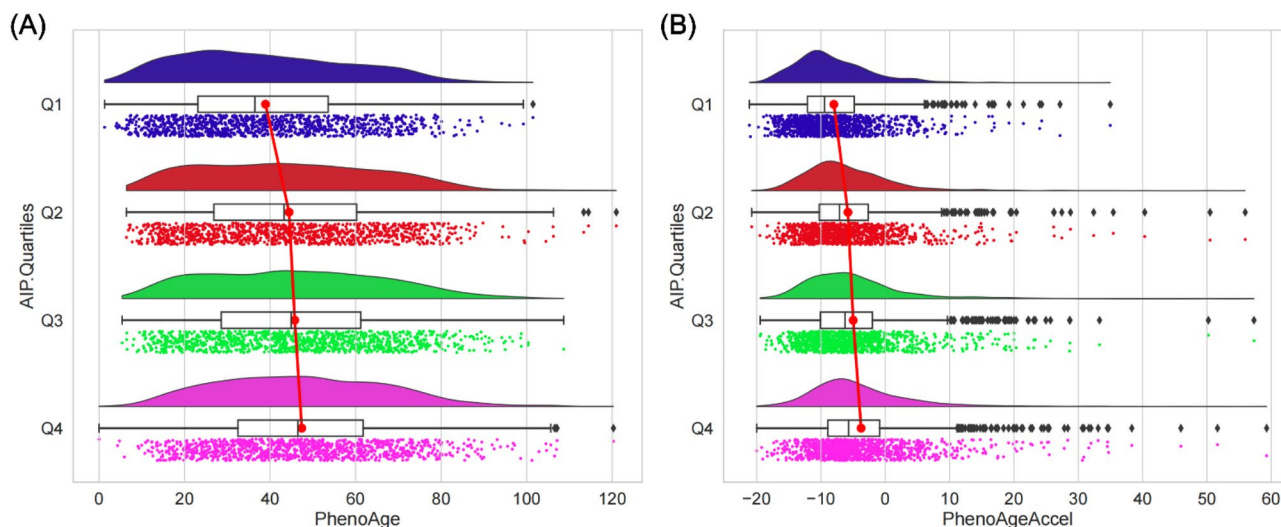


Fig. 2 Raincloud plot revealed the difference in PhenoAge and PhenoAgeAccel across AIP quartile groups. (A) PhenoAge; (B) PhenoAgeAccel. *Note:* The raincloud plot is composed of four components arranged vertically: a half-violin plot at the top, followed by a boxplot, raw data points, and connecting lines that link the means of different groups. This arrangement provides a more comprehensive view of the data

Table 2 Association between AIP and PhenoAgeAccel

Exposure	Model 1 β (95% CI) <i>P</i> value	Model 2 β (95% CI) <i>P</i> -value	Model 3 β (95% CI) <i>P</i> value
AIP	5.189 (4.453, 5.926) < 0.00001	4.886 (4.134, 5.638) < 0.00001	1.820 (1.085, 2.556) < 0.00001
AIP quartile			
Q1	0	0	0
Q2	2.186 (1.562, 2.810) < 0.00001	2.053 (1.446, 2.661) < 0.00001	1.100 (0.537, 1.663) 0.00013
Q3	3.007 (2.384, 3.630) < 0.00001	2.847 (2.234, 3.461) < 0.00001	1.178 (0.597, 1.759) 0.00007
Q4	4.237 (3.613, 4.860) < 0.00001	3.969 (3.338, 4.601) < 0.00001	1.582 (0.970, 2.194) < 0.00001
<i>P</i> for trend	< 0.00001	< 0.00001	< 0.00001

AIP, atherogenic index of plasma; CVD, cardiovascular disease; BMI, body mass index; PIR, ratio of family income to poverty; Q, quartile; PA, physical activity; PhenoAge, phenotypic age; PhenoAgeAccel, phenotypic age acceleration

Model 1: adjusted for no covariates

Model 2: adjusted for variables of age, gender, race, education, marital status, and PIR

Model 3: adjusted for variables of age, gender, race, education, marital status, PIR, BMI, diabetes, hypertension, CVD, smoking, alcohol consumption, and PA

Results

Baseline characteristics

Of the total 4,471 participants included in this study, the median chronological age was 49 (35–64) years, and the median PhenoAge was 42.85 (27.30–59.68) years, and the PhenoAgeAccel was -6.92 (-10.52 to -2.46) years. 713 individuals (15.95%) exhibited accelerated aging, indicating that they appear to be older than what they should be physiologically corresponding to their chronological age. The baseline characteristics of the study population was presented based on AIP quartiles in Table 1. In comparison to individuals in the lowest quartile of

the AIP, those in the highest quartile were more likely to be male and of Mexican American heritage. They also exhibited lower levels of PIR, engaged in less physical activity, and had higher BMI values. Furthermore, they tended to have lower educational levels, be married, were more frequently smokers and former drinkers, and had an increased likelihood of diabetes, hypertension, and CVD. Noteworthy, individuals with higher AIP showed higher levels of PhenoAge (Fig. 2A) and PhenoAgeAccel (Fig. 2B), as well as higher frequencies of aging acceleration (AIP_{Q4} vs. Q1: 22.45% vs. 9.68%) (Table 1).

Association between AIP and PhenoAgeAccel

The association between AIP and PhenoAgeAccel was presented in Table 2. AIP, when analyzed as continuous variable, was found to be significantly and positively correlated with PhenoAgeAccel in the non-adjusted model ($\beta = 5.189$, 95% CI: 4.453–5.926, $P < 0.0001$), the partially adjusted model ($\beta = 4.886$, 95% CI: 4.134–5.638, $P < 0.0001$) and the fully adjusted model ($\beta = 1.820$, 95% CI: 1.085–2.556, $P < 0.0001$) (Table 2). After AIP was classified as categorical variables (quartiles), the AIP-PhenoAgeAccel association also remained statistically significant in all regression models (all P for trend < 0.0001). In the fully adjusted model, those in the highest AIP quartile group got a 1.582-year increase ($\beta = 1.582$, 95% CI: 0.970–2.194, $P < 0.0001$) in PhenoAgeAccel as opposed to those in the lowest AIP quartile group (Table 2).

The positive AIP-PhenoAgeAccel association was further confirmed by the smooth curve fitting analysis (Fig. 3). A positive and nonlinear association between AIP and PhenoAgeAccel was identified when AIP was analyzed as a continuous variable (P for

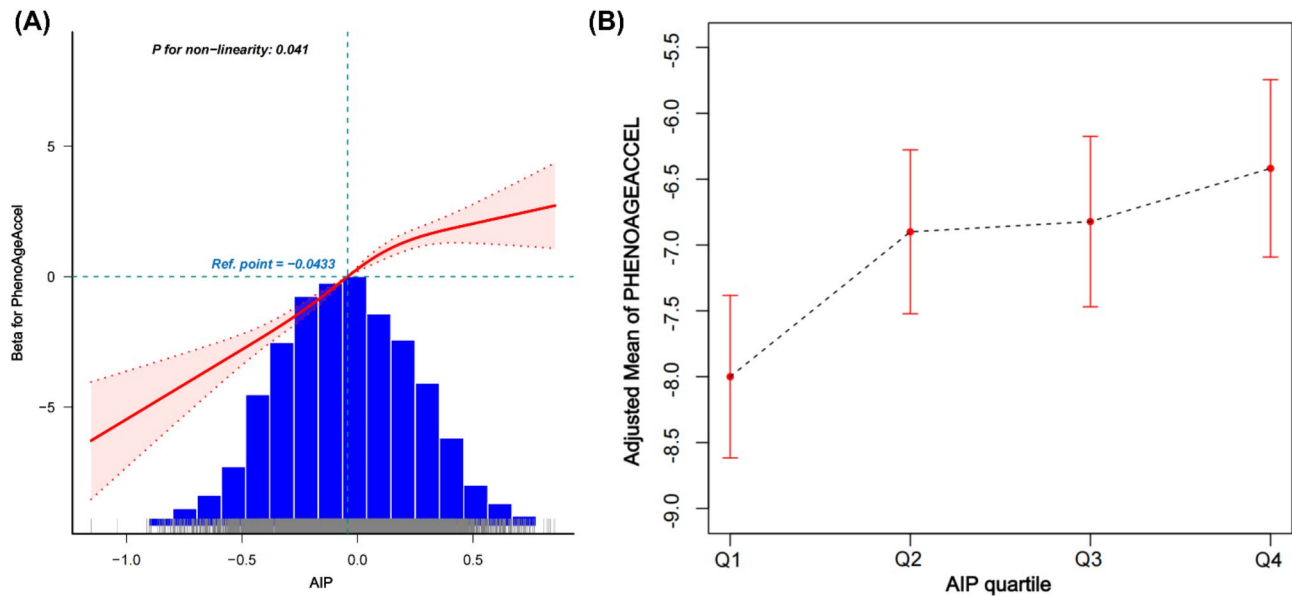


Fig. 3 Identification of the association between AIP and PhenoAgeAccel. **(A)** The association between AIP (as continuous variable) and PhenoAgeAccel by RCS analysis. The solid red line indicates the smooth curve between the beta for PhenoAgeAccel and AIP, with the red bands indicating the 95% CI of the fit. **(B)** The association between AIP (as categorical variable) and PhenoAgeAccel. The red dots reflect the adjusted mean of PhenoAgeAccel, while the line segments reflect their 95% CI

Table 3 Threshold effect analysis of AIP on PhenoAgeAccel

Outcome	β (95% CI)	P value
One—line linear regression model	5.189 (4.453, 5.926)	< 0.0001
Two—piecewise linear regression model		
Inflection point f (K)	-0.0433	
< K-segment effect 1	6.550 (5.070, 8.030)	< 0.0001
> K-segment effect 2	3.898 (2.474, 5.322)	< 0.0001
Effect size difference of 2 versus 1	-2.652 (-5.155, -0.149)	0.0379
Equation predicted values at break points	-5.348 (-5.722, -4.974)	
Log-likelihood ratio test		0.038

The results are presented as β (95% CI) and P value, and a P value lower than 0.05 indicated the statistical significance of the association. Variables of model 3 in Table 2 were adjusted.

AIP, atherogenic index of plasma.

Table 4 Association between AIP and PhenoAgeAccel based on the threshold of -0.0433 for AIP

Exposure	Model 1 β (95% CI) P value	Model 2 β (95% CI) P value	Model 3 β (95% CI) P value
AIP categorical			
< = -0.0433	0	0	0
> -0.0433	2.528 (2.085, 2.972) < 0.00001	2.291 (1.851, 2.732) < 0.00001	0.738 (0.318, 1.159) 0.00058

The variables adjusted in model 1, model 2 and model 3 were consistent with those in Table 2

AIP, atherogenic index of plasma; CVD, cardiovascular disease; BMI, body mass index; PIR, ratio of family income to poverty; Q, quartile; PA, physical activity; PhenoAge, phenotypic age; PhenoAgeAccel, phenotypic age acceleration

non-linearity = 0.041), with an inflection point of -0.0433 for AIP being determined by dose-response relationship analysis (Fig. 3A). A significant association was observed between AIP and PhenoAgeAccel before this turning point ($\beta = 6.550$, 95% CI: 5.070–8.030, $P < 0.0001$), and this relationship continued to be significantly relevant even after the turning point ($\beta = 3.898$, 95% CI: 2.474–5.322, $P < 0.0001$) (Table 3). Moreover, participants with AIP values exceeding this inflection point (> -0.0433) experienced a significant increase of 0.738 years (95% CI: 0.318–1.159, $P = 0.00058$) in PhenoAgeAccel compared to those with AIP values below -0.0433. (Table 4). Finally, RCS analysis confirmed an upward dose-response relationship across AIP quartiles, demonstrating a graded increase in PhenoAgeAccel with ascending AIP quartile categories (Fig. 3B).

Subgroup analysis

Subgroup analyses, along with interaction tests, were employed to explore the potential variations in the AIP-PhenoAgeAccel association across different subgroups stratified by gender, age, BMI, education level, marital status, PIR, as well as the presence of diabetes, hypertension, CVD, smoking, and drinking. As presented in Table 5, the results revealed that the AIP-PhenoAgeAccel association differed significantly in subgroups classified by gender, diabetes and hypertension (all P for interaction < 0.05). Specifically, for females, as well as individuals with diabetes and hypertension, an increase of one unit in AIP corresponded to an increase of 3.632 years ($\beta = 3.632$, 95% CI: 2.530–4.735), 4.933 years ($\beta = 4.933$,

Table 5 Association between AIP and PhenoAgeAccel in different subgroups

Characteristics	β (95%CI)	P value	P for interaction
Gender			0.0353
Male	1.853 (0.853 ~ 2.854)	0.0003	
Female	3.632 (2.530 ~ 4.735)	<0.0001	
AGE categorical			0.8756
<=40	2.659 (1.677 ~ 3.641)	<0.0001	
40-60	2.370 (1.085 ~ 3.655)	0.0003	
>60	2.914 (1.309 ~ 4.519)	0.0004	
BMI categorical			0.5959
<=25	2.010 (0.690 ~ 3.330)	0.0029	
25-30	1.934 (0.717 ~ 3.150)	0.0019	
>30	2.775 (1.433 ~ 4.117)	<0.0001	
Education			0.8868
Less than high school	2.552 (1.040 ~ 4.063)	0.0010	
High school or equivalent	2.382 (0.794 ~ 3.969)	0.0033	
Some college or above	2.276 (1.263 ~ 3.290)	<0.0001	
Marital status			0.6910
Married	2.063 (1.040 ~ 3.085)	<0.0001	
Never married	3.133 (1.479 ~ 4.787)	0.0002	
Others	2.435 (1.011 ~ 3.858)	0.0008	
PIR categorical			0.7723
<=1.3	2.563 (1.159 ~ 3.968)	0.0004	
1.3-3.5	2.058 (0.809 ~ 3.307)	0.0013	
>3.5	2.497 (1.268 ~ 3.726)	<0.0001	
Diabetes			0.0128
Yes	4.933 (1.387 ~ 8.480)	0.0066	
No	1.966 (1.248 ~ 2.683)	<0.0001	
Hypertension			0.0032
Yes	3.856 (2.365 ~ 5.346)	<0.0001	
No	1.612 (0.795 ~ 2.429)	0.0001	
CVD			0.0652
No	2.243 (1.477 ~ 3.009)	<0.0001	
Yes	4.272 (1.484 ~ 7.061)	0.0028	
Smoking			0.3567
Never smoker	2.416 (1.384 ~ 3.448)	<0.0001	
Former smoker	2.759 (1.283 ~ 4.235)	0.0003	
Current smoker	1.840 (0.241 ~ 3.439)	0.0243	
Alcohol consumption			0.0768
Never drinker	3.932 (1.233 ~ 6.632)	0.0045	
Former drinker	3.093 (1.104 ~ 5.081)	0.0024	
Current drinker	1.981 (1.107 ~ 2.855)	<0.0001	
Missing	-0.470 (-3.062 ~ 2.122)	0.7224	

AIP, atherogenic index of plasma; CVD, cardiovascular disease; BMI, body mass index; PIR, ratio of family income to poverty; Q, quartile; PA, physical activity; PhenoAge, phenotypic age; PhenoAgeAccel, phenotypic age acceleration. The variables adjusted for subgroup analyses were consistent with Model 3 in Table 2 except the stratifying variable.

95% CI: 1.387–8.480), and 3.856 years ($\beta = 3.856$, 95% CI: 2.365–5.346) in PhenoAgeAccel, respectively, compared to their male, non-diabetic, and non-hypertensive counterparts. Such differences in AIP-PhenoAgeAccel association were further verified by the stratified RCS analyses, as depicted in Fig. 4.

Mediation effects HOMA-IR on AIP-PhenoAgeAccel association

In light of the interconnectedness between insulin resistance, as represented by HOMA-IR, and biological aging [54, 55], additional mediation effect analyses were carried out. HOMA-IR was found to mediate 39.21% of the association between AIP and PhenoAgeAccel (Fig. 5).

Potential mechanisms and core targets involved in biological aging

So far, our results show a nonlinear AIP-PhenoAgeAccel association, with insulin resistance (HOMA-IR) serving

as a partial mediator. Since AIP is calculated from TG and HDL-C, AIP levels mirror TG/HDL-C metabolic changes regulated by key genes. Analogously, insulin resistance involves dysregulation of core glucose-homeostasis targets. Thus, to uncover the drivers of biological aging, we used network pharmacology to identify key molecular targets and pathways in accelerated aging, which may offer insights for developing anti-aging therapies.

According to the results from network pharmacological analyses, a total of 1369, 360, 5983, and 386 genes identified for cholesterol metabolism, triglyceride metabolism, insulin resistance, and biological aging, respectively. The Venn diagram revealed that 51 intersection targets were shared by the four biological processes (Fig. 6A). The STRING database was utilized to get the PPI information from these 51 genes (Fig. 6B), and the PPI network analysis was used to identify the top 10 intersection targets, which were INS, APOE, IL6, PPARG, MTOR, IL10, ACE, PPARGC1A, SERPINE1, and APOB, respectively (Fig. 6D).

GO and KEGG enrichment analyses were performed utilizing the DAVID database to delineate “core target-biological pathway” networks and unveil key pathways. The analysis revealed a total of 159 entries for biological processes (BP), 27 for cellular components (CC), and 26 for molecular functions (MF). The top 10 entries were visualized and ranked according to gene count and $\log_{10}(P)$ value). The findings indicate that the biological processes are predominantly linked to cholesterol metabolism, glucose homeostasis, regulation of signaling receptor activity, and gene expression control (Fig. 6E). In terms of cellular components, significant involvement was observed in the early endosome, lysosome, and endoplasmic reticulum lumen (Fig. 6E). Furthermore, the molecular functions highlighted critical interactions, such as binding to low-density lipoprotein receptors, very-low-density lipoprotein receptors, and various enzymes (Fig. 6E).

Similarly, the KEGG enrichment analysis performed using the DAVID data platform identified a total of 24 pathways. Based on the FDR-corrected p-values, the most significant KEGG pathways associated with these targets included the AMPK signaling pathway, cholesterol metabolism, longevity regulating pathway, insulin resistance, apelin signaling pathway, JAK-STAT signaling pathway, lipid metabolism and atherosclerosis, and the FoxO signaling pathway, among others (Fig. 6C).

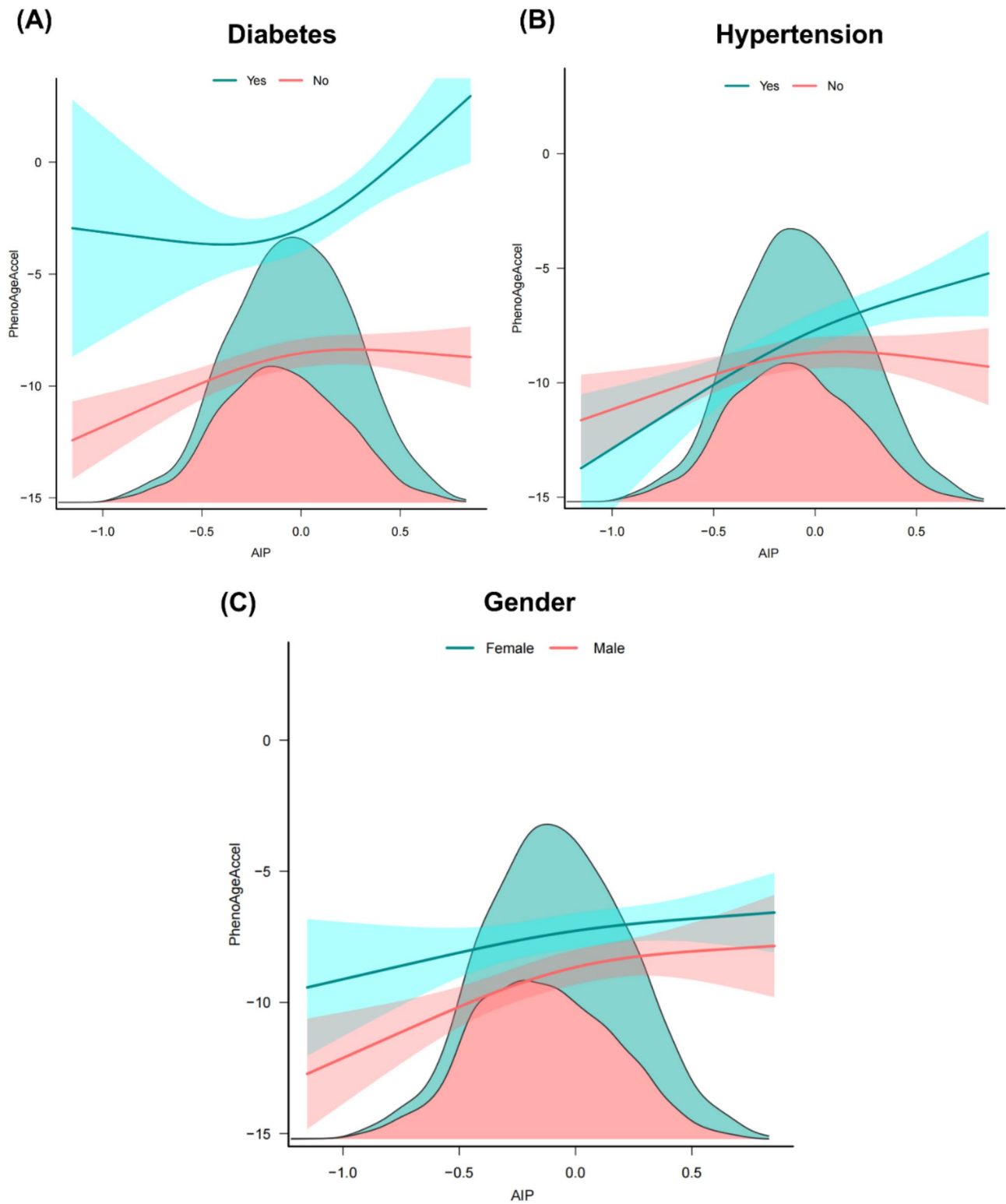


Fig. 4 Identification of the association between AIP and PhenoAgeAccel in different subgroups by RCS analysis. **(A)** RCS analysis to determine the association between AIP and PhenoAgeAccel based on stratification of diabetes. **(B)** RCS analysis to determine the association between AIP and PhenoAgeAccel based on stratification of hypertension. **(C)** RCS analysis to determine the association between AIP and PhenoAgeAccel based on stratification of gender.

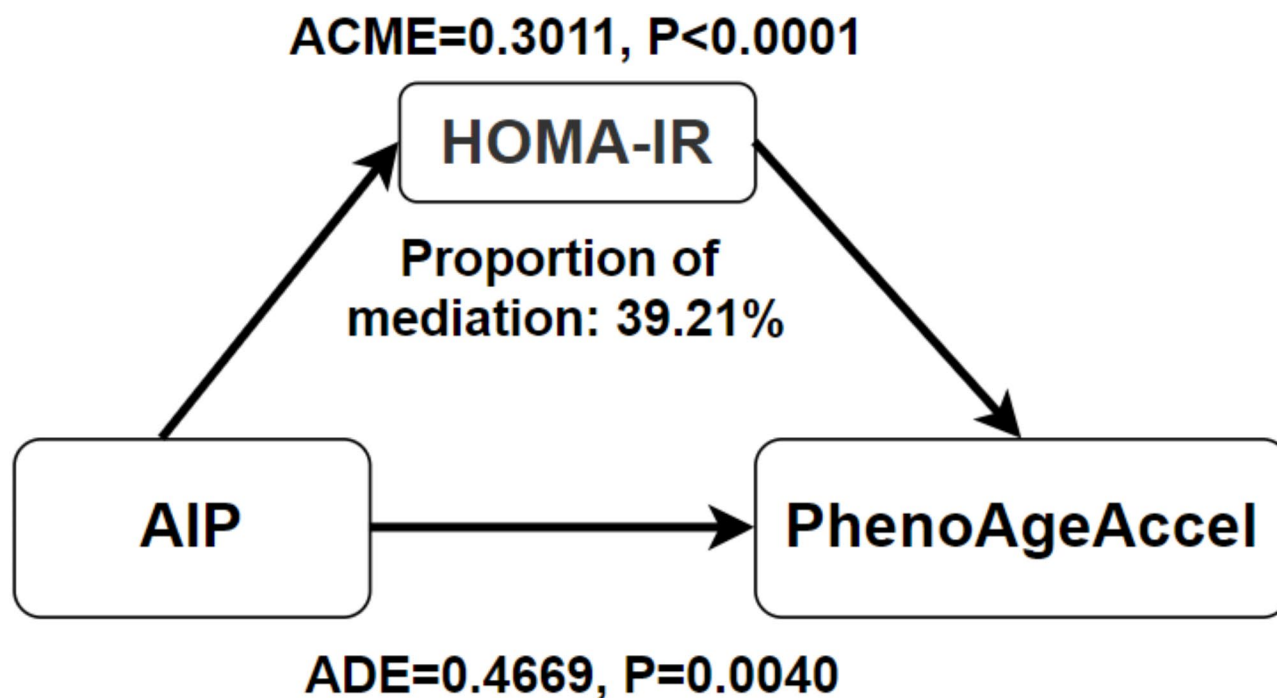


Fig. 5 HOMA-IR mediates the association of AIP with PhenoAgeAccel. *ACME*, average causal mediation effects; *ADE*, average direct effects

Discussion

In this cross-sectional analysis of 4,471 NHANES participants, we observed a significant positive association between AIP and PhenoAgeAccel. Participants in higher AIP quartiles exhibited significantly accelerated PhenoAgeAccel compared with the lowest quartile group (Q4 vs. Q1: $\beta = 1.58$ years, 95% CI: 0.970, 2.194; $P_{\text{trend}} < 0.001$) in the fully adjusted model, with the AIP-PhenoAgeAccel association being more pronounced among female and individuals with diabetes or hypertension. Moreover, adjusted RCS analysis revealed an inverse L-shaped dose–response relationship between AIP and PhenoAgeAccel. Mediation analysis further indicated that insulin resistance, quantified by HOMA-IR, accounted for 39.21% of this association. Additionally, network pharmacological analysis revealed that the core targets involved in biological aging included INS, APOE, APOB, IL6, IL10, PPARG, MTOR, ACE, PPARGC1A, SERPINE1, etc., which were functionally linked to key signaling pathways like AMPK, apelin, JAK-STAT, FoxO, and so on.

There existed some studies which provided significant insights concerning the association between lipid profiling and aging. For example, by using multi-omics methods, Eriksson et al. explored the association of aging acceleration with multi-systemic dysregulation factors (e.g., nutrition, lipid, gut microbiome) among Asian women of reproductive age [56]. A total of 132 lipid species were found to correlate with PhenoAgeAccel, within which the phosphatidylcholine(O-36:0) and

cholesteryl-ester(24:5) showing the most prominent positive and inverse association, respectively. Moreover, a longitudinal lipidomic profiling analyses based on 112 participants conducted by Michael P Snyder et al. have identified multiple significant alterations of lipid metabolites associated with aging [57], including an increase in saturated fatty acids (FAs), monounsaturated fatty acids, arachidonic acid (FA(20:4)), and lysophosphatidyl choline, and a decrease in polyunsaturated FAs, omega-3 FAs, docosahexaenoic acid (FA(22:6)), eicosapentaenoic acid (FA(20:5)), and linoleic acid (FA(18:2)). Undoubtedly, these studies have offered a deeper understanding of the molecular and metabolic mechanisms for us regarding biological aging. However, from the perspective of clinical application, several challenges should be conquered before they can be implemented in clinical practice, such as the simplicity of detection methods, affordability, robustness across diverse diseases and populations, accessibility, generalizability, and so on. Therefore, as discussed previously, the distinct advantages of AIP, including robust correlation with dyslipidemia, superior sensitivity to dynamic lipidomic alterations, and validated predictive utility across heterogeneous disease contexts and populations, suggesting that it may represent a relatively superior predictor among currently available aging indicators.

In this study, dyslipidemia (as quantified by AIP) was observed to associate with significant accelerated aging, with one unit increase in AIP leading to 1.82 year (95% CI: 1.085–2.556; $P < 0.001$) increase of PhenoAgeAccel

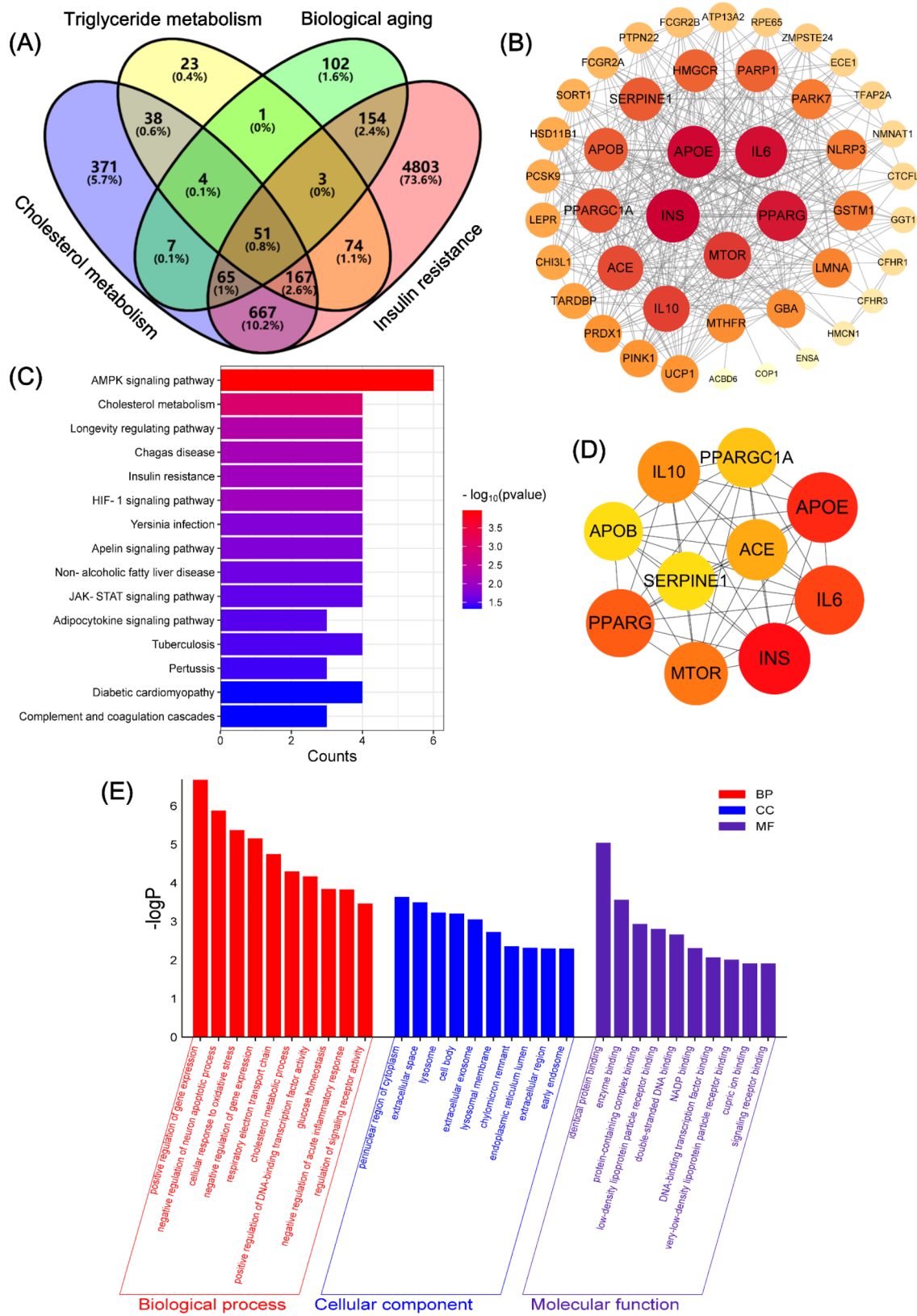


Fig. 6 (See legend on next page.)

(See figure on previous page.)

Fig. 6 Exploration of potential targets and mechanisms of cholesterol metabolism, triglyceride metabolism and insulin resistance associated with biological aging. **(A)** Venn graph revealing the intersection targets among cholesterol metabolism, triglyceride metabolism, insulin resistance and biological aging. **(B)** Protein–protein interaction (PPI) network exhibiting the associations of the overlapping targets. **(C)** PPI network showing the relationships of the top 10 intersection targets. **(D)** GO enrichment analysis based on the intersection genes. **(E)** KEGG enrichment analysis based on the intersection genes.

in the fully adjusted model. The mechanisms underlying the association between dyslipidemia and accelerated aging are complex and multifaceted, but some pivotal evidences from previous studies can provide reasonable explanations. Firstly, dyslipidemia can contribute to the accumulation of intracellular lipid which in turn induces cellular senescence [58, 59]. For example, pretreatment of C75 (an inhibitor of fatty acid synthase) in mouse and human cells was proved to prevent the induction of cellular senescence, as indicated by the reduced expression of SASP factors, such as IL-1 α , IL-1 β and IL-6 [58]. Another piece of direct supporting evidence is that accumulation of glycerol-3-phosphate (G3P, a precursor of triglyceride synthesis) in fibroblasts via activating p53-dependent glycerol kinase and inactivating phosphocytidyltransferase 2 (PCYT2) could trigger the expression of SASP genes and thus the senescence of juvenile fibroblasts [59]. These facts, from the perspective of cellular lipid metabolism, directly confirm the casual link between dyslipidemia and aging. Furthermore, dyslipidemia may elicit accelerated aging via reducing telomeres in multiple tissues, such as leukocytes [20, 60, 61], saliva [62], whole blood samples [63], and so on. Mechanistically, dyslipidemia could induce telomere shortening via multiple mechanisms, including oxidative stress, abnormal signaling pathways (e.g., mTOR, PPAR γ), release of inflammatory cytokines (e.g., TNF- α , IL-6), insulin signaling pathway irregularities, and epigenetic regulation [64–67]. Additionally, dyslipidemia can also induce lipid toxicity via lipid peroxidation, resulting in organelle dysfunction (e.g., mitochondria damage, lysosome dysfunction, endoplasmic reticulum stress) and ultimately cellular aging [64–69]. Collectively, these findings, combined with the link between lipidomic profiles and aging discussed earlier, confirmed the pivotal role of dyslipidemia in accelerating aging.

In this study, we identified a nonlinear correlation between AIP and PhenoAgeAccel. Notably, we observed that the absolute beta coefficient of PhenoAgeAccel was lower at high AIP levels compared to that within low AIP levels. This suggests that compensatory mechanisms (e.g., autophagy activation or upregulation of antioxidant enzymes) may be triggered at elevated AIP levels, partially counteracting the damage caused by dyslipidemia, thereby weakening the association between AIP and accelerated aging. The following speculations may provide potential explanations for this phenomenon. Firstly, previous studies have shown that dyslipidemia

can induce lipotoxic stress, which may compensatorily activate autophagy via the KEAP1-NFE2L2 pathway [70], thus alleviating lipid toxicity and possibly cellular senescence. Furthermore, heightened lipotoxic stress induced by dyslipidemia could contribute to the increase of intracellular oxidative stress levels, which may trigger compensatory activation of antioxidant enzyme systems (e.g., glutathione, SOD) to maintain cellular homeostasis [71]. This may represent another mechanism that weakens AIP-PhenoAgeAccel association. Additionally, given the strong association between AIP and insulin resistance [28], elevated AIP levels may amplify the mediating effects of insulin resistance, thereby attenuating the direct impact of AIP on aging acceleration.

In this study, subgroup analyses revealed that the nonlinear positive association between the AIP and PhenoAgeAccel was significantly stronger in females and individuals with diabetes and hypertension. This phenomenon might be understood as follows. Firstly, substantial evidence indicates significant gender differences in lipid profiles throughout life, with females experiencing greater fluctuations in triglyceride and LDL-C levels due to factors such as the menstrual cycle, pregnancy, breastfeeding, and menopause [72]. During these phases, women often exhibit a more adverse lipid profile (higher LDL-C and triglyceride levels) than men, potentially contributing to accelerated aging as they age. Moreover, abundant evidence shows that a high glucose environment in diabetic individuals can induce premature cellular senescence and promote inflammatory cytokine production [73–75], thus inducing accelerating aging. This may account for the differences in the AIP-PhenoAgeAccel association between diabetic and non-diabetic individuals. Additionally, it is evident that increased premature aging and senescence contribute to the development of hypertension, while hypertension can, in turn, induce premature aging and senescence [76]. This reciprocal relationship may explain why hypertensive individuals exhibit a stronger AIP-PhenoAgeAccel association than non-hypertensive individuals.

Our study observed a mediation proportion of 39.21% for HOMA-IR between AIP and accelerated aging, which aligns with previous findings. The mediation proportion reflects the relative contribution of IR to accelerated aging driven by dyslipidemia. The value of 39.21% suggests that besides IR, other mechanisms related to dyslipidemia (e.g., inflammation and oxidative stress) may collectively drive the aging process, which is consistent

with the multifactorial-driven characteristics of aging, indicating that IR is an critical but not the exclusive drivers of aging acceleration. Previous studies have revealed that the mediation proportion of IR in metabolism-related diseases typically ranges from 7 to 80%. For instance, Liu et al. [77] found mediation proportions of HOMA-IR for PhenoAgeAccel were 6.9% (VFA-PhenoAgeAccel) and 13.4% (SFA-PhenoAgeAccel) in the 18–44 aged group. Similarly, a mediation proportion of 51.7% and 11.14% was reported by Li et al. [78] and Huang et al. [79] in sarcopenia and gout populations, respectively. The current result (39.21%) falls within this range, further supporting its biological plausibility. Additionally, the findings from previous studies also supported the results in our study that IR mediates aging acceleration caused by dyslipidemia. In human studies, elevated triglycerides and its metabolites (free fatty acids, FFAs) were found to closely correlate with IR [80]. FFAs were proved to induce IR in humans by inhibiting glucose transport/phosphorylation, which then reduced the rate of muscle glycogen synthesis and glucose oxidation [81]. Also, high-fat diets which induced dyslipidemia in animal models were proved to induce IR via modulating pathways like DAG/PKC, ceramide/Akt/PKB [82], and so on. Actually, IR has been already confirmed as one of the core drivers for accelerating aging process by various studies [83–85], which can be supported by the facts that interventions aimed at alleviating IR (e.g., metformin [86], exercise [87]) can significantly attenuate the hallmarks of aging. These evidences collectively explained the rationality of IR as a crucial mediator in dyslipidemia-induced accelerated aging.

Network pharmacology is a holistic research method based on system biology theory, which exhibits significant advantages in identifying core targets of disease/drug and screening key mechanisms. Some pivotal findings were identified via network pharmacological analysis in this study. Firstly, through topological analysis of network pharmacology, we identified core targets (e.g., IL6, IL10) associated with dyslipidemia-related accelerated aging. These targets may not only represent novel biomarkers for accelerated aging, but also core therapeutic targets for developing anti-aging drugs. Furthermore, the PPI network analysis of network pharmacology helped us identify key hub genes (e.g., ACE) not directly covered by keywords. Notably, ACE is a well-established therapeutic target for hypertension, suggesting a potential link between hypertension and accelerated aging, as well as the anti-aging effects of ACE inhibitors. In this study, we found that hypertensive patients exhibited higher PhenoAgeAccel values at equivalent AIP levels, strongly supporting this speculation. Additionally, we found some

pivotal pathways (i.e., infection-related pathways) which were not directly associated with keywords, including chagas disease, yersinia infection, tuberculosis, pertussis, staphylococcus aureus infection, amoebiasis, and coronavirus disease (COVID-19). These findings suggest that dyslipidemia may not only associate with accelerated aging but also correlate with increased susceptibility to pathogens. Actually, previous studies have reported that cholesterol alterations in macrophage lead to impaired bactericidal function and exacerbated bone destruction [88]. This implies that for chronic infection patients with dyslipidemia (e.g., chronic osteomyelitis), lipid metabolism-regulating drugs may need to be integrated into the comprehensive treatment strategy.

Our study represents the first to uncover a positive and nonlinear association between AIP and PhenoAgeAccel. The strengths of our study can be manifested by several key aspects. Firstly, our research utilized a sophisticated multi-stage probability sampling design involving a large population, which significantly enhances the reliability of our findings. Secondly, the data collection procedures and blood sample tests were carried out by trained professionals, thereby substantially reducing potential bias in these aspects. Thirdly, we employed a range of advanced statistical methods to rigorously validate the relationship between AIP and PhenoAgeAccel. This included linear regression models, subgroup analyses, interaction tests, restricted cubic spline analyses, and network pharmacological analysis, allowing us to examine the association from multiple perspectives.

Despite the strengths of our study, several limitations should be acknowledged. Firstly, the cross-sectional nature of the NHANES data impedes our ability to establish a causal link between AIP and PhenoAgeAccel. As a result, future research could employ longitudinal or experimental designs to investigate the causal relationship. Secondly, network pharmacology-based gene analyses are inherently influenced by data source heterogeneity and sample variability. Notably, the hub genes linked to cholesterol metabolism, triglyceride metabolism, biological aging and insulin resistance identified in GeneCards likely represent aggregated findings from heterogeneous studies across diverse populations and regions. While providing preliminary insights, these findings require rigorous experimental validation to establish generalizability. Thirdly, the exclusive focus of this study on the US population intrinsically restricts the generalizability of the findings across distinct geographical regions and ethnic groups. Therefore, future research is warranted to validate the external validity of these conclusions through multi-regional cohort studies that engage

diverse populations. Fourth, the use of self-reported data (such as physical activity, smoking, and alcohol consumption) may introduce potential bias into this study. Fifth, given that biological aging is a multifactorial process driven by complex mechanisms, a multidimensional approach is essential for constructing comprehensive aging indicators. While the AIP demonstrated a significant association with accelerated aging in this study, it primarily reflects dyslipidemia-related aspects. To enhance the accuracy and specificity of accelerated aging assessment, future studies should consider integrating AIP with complementary aging indicators, such as DNA methylation age, telomere length, and frailty indices, within a unified evaluation framework. Additionally, despite adjusting for potential confounders in our analysis, unmeasured factors (e.g., genetic predispositions, dietary influences, environmental conditions) may also impact the AIP-PhenoAgeAccel relationship. Finally, the inability to calculate other aging biomarkers (e.g., DNA methylation age, GrimAge, metabolic age score) from NHANES data hinders evaluating AIP's associations with other aging indicators.

Our findings can offer valuable references for clinical practice and public health endeavors. Clinically, the AIP may serve as a key marker for assessing the risk of accelerated aging. Measuring AIP levels enables healthcare professionals to identify populations at high risk of aging and susceptibility to age-related diseases, facilitating the timely use of intervention strategies. From a public health perspective, AIP's notable advantages in terms of ease of monitoring, accessibility, and affordability can assist the general population in better understanding their health status and disease susceptibility.

In summary, our study demonstrates that monitoring AIP levels represents an effective approach for evaluating the risk of accelerated aging. Maintaining AIP within an optimal range may positively influence the rate of aging and help prevent age-related diseases. While additional research is necessary to clarify the underlying mechanisms, our findings provide valuable insights that may help to formulate effective prevention strategies.

Conclusion

In this study, we found that PhenoAgeAccel increased with rising AIP levels, a trend that was particularly pronounced in female, diabetic, and hypertensive individuals. Additionally, the relationship between AIP and PhenoAgeAccel exhibited an inverse L-shaped pattern, which was mediated by insulin resistance as indicated by HOMA-IR. Our findings indicated that AIP levels may offer valuable information regarding aging acceleration and susceptibility to age-related diseases.

Supplementary Information

The online version contains supplementary material available at <https://doi.org/10.1186/s12933-025-02695-8>.

Supplementary Material 1

Acknowledgments

We express our gratitude to all the volunteers for their participation and to the personnel for their invaluable contributions to the NHANES study.

Author contributions

All authors have made significant contributions to this study. Fei Luo supervised the entire research process, from formulating the research design to performing data analysis and guiding the writing of the article. QianKun Yang undertook the statistical analysis, interpretation of results, revision of the initial manuscript, and completion of the revised manuscript. Li Zhang assisted in conducting data extraction, cleaning and analysis. XianJie Zhu wrote the initial manuscript for this study. All authors have approved the final version for publication and have agreed to be accountable for all aspects of the work.

Funding

This study was supported by the outstanding talent pool key support object projects of Army Medical University (Number: XZ-2019-505-021), the project of Military key clinical specialty (Number: 51561Z23711), and the 2025 Project supported by Baiqing Academic Talents Cultivation Fund of the First Affiliated Hospital of Army Military Medical University (Southwest Hospital) (Number: 2025BQCX-26).

Availability of data and materials

This study analyzed publicly available datasets, which can be accessed at the following link: <https://www.cdc.gov/nchs/nhanes/index.htm>.

Declarations

Ethics approval and consent to participant

The program was approved by the National Center for Health Statistics Ethics Review Board. All of the participants provided written informed consent. No additional ethical review board approval was required to analyze the anonymized NHANES data.

Consent for publication

Not applicable.

Competing interests

The authors declared that no potential conflicts of interests existed in this study.

Author details

¹National & Regional United Engineering Lab of Tissue Engineering, Department of Orthopedics, Southwest Hospital, Army Medical University, No.29 Gaotanyan St., Shapingba District, Chongqing 400038, China

²Graduate School of Dalian Medical University, Dalian 116000, China

³Department of Hematology, National Clinical Research Center for Child Health and Disorders, Ministry of Education Key Laboratory of Child Development and Disorders, Chongqing Key Laboratory of Pediatrics, Children's Hospital of Chongqing Medical University, No.136 of Zhong Shan Second Road, Yu Zhong District, Chongqing 400014, China

⁴Department of Neurology, National Clinical Research Center for Child Health and Disorders, Ministry of Education Key Laboratory of Child Development and Disorders, Chongqing Key Laboratory of Pediatrics, Children's Hospital of Chongqing Medical University, No.136 of Zhong Shan Second Road, Yu Zhong District, Chongqing 400014, China

Received: 23 December 2024 / Accepted: 17 March 2025

Published online: 25 April 2025

References

- Liu Z, Kuo P-L, Horvath S, Crimmins E, Ferrucci L, Levine M. A new aging measure captures morbidity and mortality risk across diverse subpopulations from NHANES IV: A cohort study. *PLoS Med.* 2018;15:e1002718.
- Ferrucci L, Hesdorffer C, Bandinelli S, Simonsick EM. Frailty as a nexus between the biology of aging, environmental conditions and clinical geriatrics. *Public Health Rev.* 2010;32:475–88.
- Noroozi R, Ghafouri-Fard S, Pisarek A, Rudnicka J, Spólnicka M, Branicki W, et al. DNA methylation-based age clocks: from age prediction to age reversion. *Ageing Res Rev.* 2021;68:101314.
- Benetos A, Okuda K, Lajemi M, Kimura M, Thomas F, Skurnick J, et al. Telomere length as an indicator of biological aging: the gender effect and relation with pulse pressure and pulse wave velocity. *Hypertension.* 2001;37:381–5.
- Belsky DW, Moffitt TE, Cohen AA, Corcoran DL, Levine ME, Prinz JA, et al. Eleven telomere, epigenetic clock, and biomarker-composite quantifications of biological aging: Do they measure the same thing? *Am J Epidemiol.* 2018;187:1220–30.
- Marioni RE, Shah S, McRae AF, Ritchie SJ, Muniz-Terrera G, Harris SE, et al. The epigenetic clock is correlated with physical and cognitive fitness in the Lothian Birth Cohort 1936. *Int J Epidemiol.* 2015;44:1388–96.
- Chen BH, Marioni RE, Colicino E, Peters MJ, Ward-Caviness CK, Tsai P-C, et al. DNA methylation-based measures of biological age: meta-analysis predicting time to death. *Aging (Albany NY).* 2016;8:1844–59.
- Horvath S, Gurven M, Levine ME, Trumble BC, Kaplan H, Allayee H, et al. An epigenetic clock analysis of race/ethnicity, sex, and coronary heart disease. *Genome Biol.* 2016;17:171.
- Mitnitski AB, Mogilner AJ, Rockwood K. Accumulation of deficits as a proxy measure of aging. *ScientificWorldJournal.* 2001;1:323–36.
- Levine ME. Modeling the rate of senescence: Can estimated biological age predict mortality more accurately than chronological age? *J Gerontol A Biol Sci Med Sci.* 2013;68:667–74.
- Levine ME, Lu AT, Quach A, Chen BH, Assimes TL, Bandinelli S, et al. An epigenetic biomarker of aging for lifespan and healthspan. *Aging (Albany NY).* 2018;10:573–91.
- Finkel D, Whitfield K, McGue M. Genetic and environmental influences on functional age: a twin study. *J Gerontol B Psychol Sci Soc Sci.* 1995;50:P104–113.
- Ma Z, Zhu C, Wang H, Ji M, Huang Y, Wei X, et al. Association between biological aging and lung cancer risk: cohort study and Mendelian randomization analysis. *iScience.* 2023;26:106018.
- Li X, Cao X, Zhang J, Fu J, Mohedaner M, Danzengzhuoga, et al. Accelerated aging mediates the associations of unhealthy lifestyles with cardiovascular disease, cancer, and mortality. *J Am Geriatr Soc.* 2024;72:181–93.
- Ruan Z, Li D, Huang D, Liang M, Xu Y, Qiu Z, et al. Relationship between an ageing measure and chronic obstructive pulmonary disease, lung function: a cross-sectional study of NHANES, 2007–2010. *BMJ Open.* 2023;13:e076746.
- Cui F, Tang L, Li D, Ma Y, Wang J, Xie J, et al. Early-life exposure to tobacco, genetic susceptibility, and accelerated biological aging in adulthood. *Sci Adv.* 2024;10:747.
- Liu C, Hua L, Xin Z. Synergistic impact of 25-hydroxyvitamin D concentrations and physical activity on delaying aging. *Redox Biol.* 2024;73:103188.
- Bischoff-Ferrari HA, Gängler S, Wiecek M, Belsky DW, Ryan J, Kressig RW, et al. Individual and additive effects of vitamin D, omega-3 and exercise on DNA methylation clocks of biological aging in older adults from the DO-HEALTH trial. *Nat Aging.* 2025;5(3):376–85.
- Luo S, Wong ICK, Chui CSL, Zheng J, Huang Y, Schooling CM, et al. Effects of putative metformin targets on phenotypic age and leukocyte telomere length: a Mendelian randomisation study using data from the UK Biobank. *Lancet Healthy Longev.* 2023;4:e337–44.
- Aulinas A, Ramirez M-J, Barahona M-J, Valassi E, Resmini E, Mato E, et al. Dyslipidemia and chronic inflammation markers are correlated with telomere length shortening in Cushing's syndrome. *PLoS ONE.* 2015;10:e0120185.
- Yan S, Luo W, Lei L, Zhang Q, Xiu J. Association between serum Klotho concentration and hyperlipidemia in adults: a cross-sectional study from NHANES 2007–2016. *Front Endocrinol (Lausanne).* 2023;14:1280873.
- Liu H-H, Li J-J. Aging and dyslipidemia: A review of potential mechanisms. *Ageing Res Rev.* 2015;19:43–52.
- Ouchi G, Komiya I, Taira S, Wakugami T, Ohya Y. Triglyceride/low-density-lipoprotein cholesterol ratio is the most valuable predictor for increased small, dense LDL in type 2 diabetes patients. *Lipids Health Dis.* 2022;21:4.
- Yu B, Li M, Yu Z, Zheng T, Feng X, Gao A, et al. The non-high-density lipoprotein cholesterol to high-density lipoprotein cholesterol ratio (NHHR) as a predictor of all-cause and cardiovascular mortality in US adults with diabetes or prediabetes: NHANES 1999–2018. *BMC Med.* 2024;22:317.
- Chen M, Chen Z, Ye H, Cheng Y, Jin Z, Cai S. Long-term association of remnant cholesterol with all-cause and cardiovascular disease mortality: a nationally representative cohort study. *Front Cardiovasc Med.* 2024;11:1286091.
- Dobiášová M, Frohlich J. The plasma parameter log (TG/HDL-C) as an atherogenic index: correlation with lipoprotein particle size and esterification rate in apoB-lipoprotein-depleted plasma (FER(HDL)). *Clin Biochem.* 2001;34:583–8.
- Li Y-W, Kao T-W, Chang P-K, Chen W-L, Wu L-W. Atherogenic index of plasma as predictors for metabolic syndrome, hypertension and diabetes mellitus in Taiwan citizens: a 9-year longitudinal study. *Sci Rep.* 2021;11:9900.
- Yin B, Wu Z, Xia Y, Xiao S, Chen L, Li Y. Non-linear association of atherogenic index of plasma with insulin resistance and type 2 diabetes: a cross-sectional study. *Cardiovasc Diabetol.* 2023;22:157.
- Tan M, Zhang Y, Jin L, Wang Y, Cui W, Nasifu L, et al. Association between atherogenic index of plasma and prehypertension or hypertension among normoglycemia subjects in a Japan population: a cross-sectional study. *Lipids Health Dis.* 2023;22:87.
- You F-F, Gao J, Gao Y-N, Li Z-H, Shen D, Zhong W-F, et al. Association between atherogenic index of plasma and all-cause mortality and specific-mortality: a nationwide population-based cohort study. *Cardiovasc Diabetol.* 2024;23:276.
- Liu Z, Zhang L, Wang L, Li K, Fan F, Jia J, et al. The predictive value of cumulative atherogenic index of plasma (AIP) for cardiovascular outcomes: a prospective community-based cohort study. *Cardiovasc Diabetol.* 2024;23:264.
- Chen M, Fang C, Guo J, Pang L, Zhou Y, Hong Y, et al. Predictive value of atherogenic index of plasma and atherogenic index of plasma combined with low-density lipoprotein cholesterol for the risk of acute myocardial infarction. *Front Cardiovasc Med.* 2023;10:1117362.
- Min Q, Wu Z, Yao J, Wang S, Duan L, Liu S, et al. Association between atherogenic index of plasma control level and incident cardiovascular disease in middle-aged and elderly Chinese individuals with abnormal glucose metabolism. *Cardiovasc Diabetol.* 2024;23:54.
- Duiyimuhan G, Maimaiti N. The association between atherogenic index of plasma and all-cause mortality and cardiovascular disease-specific mortality in hypertension patients: a retrospective cohort study of NHANES. *BMC Cardiovasc Disord.* 2023;23:452.
- Zhang Y, Li S, Wu W, Zhao Y, Han J, Tong C, et al. Machine-learning-based models to predict cardiovascular risk using oculomics and clinic variables in KNHANES. *BioData Min.* 2024;17:12.
- Zhang J, Suo Y, Wang L, Liu D, Jia Y, Fu Y, et al. Association between atherogenic index of plasma and gestational diabetes mellitus: a prospective cohort study based on the Korean population. *Cardiovasc Diabetol.* 2024;23:237.
- Shi Y, Wen M. Sex-specific differences in the effect of the atherogenic index of plasma on prediabetes and diabetes in the NHANES 2011–2018 population. *Cardiovasc Diabetol.* 2023;22:19.
- Yang H, Gong R, Liu M, Deng Y, Zheng X, Hu T. HOMA-IR is positively correlated with biological age and advanced aging in the US adult population. *Eur J Med Res.* 2023;28:470.
- Xu C, Song Z, Wang J, Li C. Association of visceral adiposity index with phenotypic age acceleration: insight from NHANES 1999–2010. *J Nutr Health Aging.* 2024;28:100323.
- Xie R, Xiao M, Li L, Ma N, Liu M, Huang X, et al. Association between SII and hepatic steatosis and liver fibrosis: a population-based study. *Front Immunol.* 2022;13:925690.
- Curtin LR, Mohadjer LK, Dohmann SM, Montaquila JM, Kruszán-Moran D, Mirel LB, et al. The national health and nutrition examination survey: sample design, 1999–2006. *Vital Health Stat.* 2012;2:1–39.
- Zhang H, Zhang G, Fu J. Exploring the L-shaped relationship between atherogenic index of plasma and depression: results from NHANES 2005–2018. *J Affect Disord.* 2024;359:133–9.
- Zhang G, Zhang H, Fu J, Zhao Y. Atherogenic index of plasma as a mediator in the association between body roundness index and depression: insights from NHANES 2005–2018. *Lipids Health Dis.* 2024;23:183.
- Son D-H, Lee HS, Lee Y-J, Lee J-H, Han J-H. Comparison of triglyceride-glucose index and HOMA-IR for predicting prevalence and incidence of metabolic syndrome. *Nutr Metab Cardiovasc Dis.* 2022;32:596–604.

45. Dai W, Zhang D, Wei Z, Liu P, Yang Q, Zhang L, et al. Whether weekend warriors (WWs) achieve equivalent benefits in lipid accumulation products (LAP) reduction as other leisure-time physical activity patterns? -Results from a population-based analysis of NHANES 2007–2018. *BMC Public Health*. 2024;24:1550.
46. Tao X, Xu X, Xu Y, Yang Q, Yang T, Zhou X, et al. Association between physical activity and visceral adiposity index (VAI) in U.S. population with overweight or obesity: a cross-sectional study. *BMC Public Health*. 2024;24:2314.
47. Xue H, Zou Y, Yang Q, Zhang Z, Zhang J, Wei X, et al. The association between different physical activity (PA) patterns and cardiometabolic index (CMI) in US adult population from NHANES (2007–2016). *Heliyon*. 2024;10:e28792.
48. Zhang Q, Xiao S, Jiao X, Shen Y. The triglyceride-glucose index is a predictor for cardiovascular and all-cause mortality in CVD patients with diabetes or pre-diabetes: evidence from NHANES 2001–2018. *Cardiovasc Diabetol*. 2023;22:279.
49. Cai Y, Chen M, Zhai W, Wang C. Interaction between trouble sleeping and depression on hypertension in the NHANES 2005–2018. *BMC Public Health*. 2022;22:481.
50. Yan J, Sun H, Xin X, Huang T. Association and mechanism of montelukast on depression: a combination of clinical and network pharmacology study. *J Affect Disord*. 2024;360:214–20.
51. NHANES Tutorials - Weighting Module [Internet]. [cited 2025 Feb 27]. Available from: <https://www.cdc.gov/nchs/nhanes/tutorials/weighting.aspx>
52. Zheng Y, Liu W, Zhu X, Xu M, Lin B, Bai Y. Associations of dietary inflammation index and composite dietary antioxidant index with preserved ratio impaired spirometry in US adults and the mediating roles of triglyceride-glucose index: NHANES 2007–2012. *Redox Biol*. 2024;76:103334.
53. Valente MJ, Rijnhart JJM, Smyth HL, Muniz FB, MacKinnon DP. Causal mediation programs in R, Mplus, SAS, SPSS, and Stata. *Struct Equ Modeling*. 2020;27:975–84.
54. Kurauchi MA, Soares GM, Marmentini C, Bronczek GA, Branco RCS, Boschero AC. Insulin and aging. *Vitam Horm*. 2021;115:185–219.
55. Kolb H, Kempf K, Martin S. Insulin and aging—a disappointing relationship. *Front Endocrinol (Lausanne)*. 2023;14:1261298.
56. Chen L, Tan KM-L, Xu J, Mishra P, Mir SA, Gong M, et al. Exploring multi-omics and clinical characteristics linked to accelerated biological aging in Asian women of reproductive age: insights from the S-PRESTO study. *Genome Med*. 2024;16:128.
57. Hornburg D, Wu S, Moqri M, Zhou X, Contrepois K, Bararpour N, et al. Dynamic lipidome alterations associated with human health, disease and ageing. *Nat Metab*. 2023;5:1578–94.
58. Fafián-Labora J, Carpintero-Fernández P, Jordan SJD, Shikh-Bahaei T, Abdullah SM, Mahenthiran M, et al. FASN activity is important for the initial stages of the induction of senescence. *Cell Death Dis*. 2019;10:318.
59. Tighanimine K, Nabuco Leva Ferreira Freitas JA, Nemazany I, Bankolé A, Benarroch-Popivker D, Brodesser S, et al. A homeostatic switch causing glycerol-3-phosphate and phosphoethanolamine accumulation triggers senescence by rewiring lipid metabolism. *Nat Metab*. 2024;6:323–42.
60. Liu X, Ma T, Yang C, Li J, Zhang Y, Zhao Y. Persistent dyslipidemia increases the longitudinal changes in telomere length. *Lipids Health Dis*. 2023;22:173.
61. Subedi P, Palma-Gudiel H, Fiehn O, Best LG, Lee ET, Howard BV, et al. Lipidomics profiling of biological aging in American Indians: the Strong Heart Family Study. *Geroscience*. 2023;45:359–69.
62. Ojeda-Rodríguez A, Zazpe I, Alonso-Pedrero L, Zalba G, Guillen-Grima F, Martínez-González MA, et al. Association between diet quality indexes and the risk of short telomeres in an elderly population of the SUN project. *Clin Nutr*. 2020;39:2487–94.
63. Novau-Ferré N, Rojas M, Gutiérrez-Tordera L, Arcelin P, Folch J, Papandreou C, et al. Lipoprotein particle profiles associated with telomere length and telomerase complex components. *Nutrients*. 2023;15:2624.
64. Zeng Q, Gong Y, Zhu N, Shi Y, Zhang C, Qin L. Lipids and lipid metabolism in cellular senescence: emerging targets for age-related diseases. *Ageing Res Rev*. 2024;97:102294.
65. Rossiello F, Jurk D, Passos JF, d'Adda di Fagagna F. Telomere dysfunction in ageing and age-related diseases. *Nat Cell Biol*. 2022;24:135–47.
66. López-Otín C, Blasco MA, Partridge L, Serrano M, Kroemer G. Hallmarks of aging: an expanding universe. *Cell*. 2023;186:243–78.
67. Shim HS, Iaconelli J, Shang X, Li J, Lan ZD, Jiang S, et al. TERT activation targets DNA methylation and multiple aging hallmarks. *Cell*. 2024;187:4030–4042.e13.
68. Lehallier B, Gate D, Schaum N, Nanasi T, Lee SE, Yousef H, et al. Undulating changes in human plasma proteome profiles across the lifespan. *Nat Med*. 2019;25:1843–50.
69. Sun X, Shen J, Perrimon N, Kong X, Wang D. The endoribonuclease Arlr1 is required to maintain lipid homeostasis by downregulating lipolytic genes during aging. *Nat Commun*. 2023;14:6254.
70. Lee DH, Park JS, Lee YS, Han J, Lee D-K, Kwon SW, et al. SQSTM1/p62 activates NFE2L2/NRF2 via ULK1-mediated autophagic KEAP1 degradation and protects mouse liver from lipotoxicity. *Autophagy*. 2020;16:1949–73.
71. Valko M, Leibfritz D, Moncol J, Cronin MTD, Mazur M, Telser J. Free radicals and antioxidants in normal physiological functions and human disease. *Int J Biochem Cell Biol*. 2007;39:44–84.
72. Holven KB, van Lennep JR. Sex differences in lipids: a life course approach. *Atherosclerosis*. 2023;384:117270.
73. Bucala R. Diabetes, aging, and their tissue complications. *J Clin Invest*. 2014;124:1887–8.
74. Monnier VM, Taniguchi N. Advanced glycation in diabetes, aging and age-related diseases: conclusions. *Glycoconj J*. 2016;33:691–2.
75. Shakeri H, Lemmens K, Gevaert AB, De Meyer GRY, Segers VFM. Cellular senescence links aging and diabetes in cardiovascular disease. *Am J Physiol Heart Circ Physiol*. 2018;315:H448–62.
76. Afsar B, Afsar RE. Hypertension and cellular senescence. *Biogerontology*. 2023;24:457–78.
77. Liu Y, Xu M, Wang L, Meng L, Li M, Mu S. The association of visceral and subcutaneous fat areas with phenotypic age in non-elderly adults, mediated by HOMA-IR and HDL-C. *Lipids Health Dis*. 2025;24:22.
78. Li M, Ji R, Liu X, Wu Y. Associations of metabolic syndrome and its components with sarcopenia, and the mediating role of insulin resistance: findings from NHANES database. *BMC Endocr Disord*. 2024;24:203.
79. Huang Y, Li Y, Wu Z, Liang Y, He J. Exploring the associations and potential mediators between lipid biomarkers and the risk of developing gout: NHANES 2007–2018. *Lipids Health Dis*. 2024;23:363.
80. Stefan N, Häring H-U. Circulating fetuin-A and free fatty acids interact to predict insulin resistance in humans. *Nat Med*. 2013;19:394–5.
81. Roden M, Price TB, Perseghin G, Petersen KF, Rothman DL, Cline GW, et al. Mechanism of free fatty acid-induced insulin resistance in humans. *J Clin Invest*. 1996;97:2859–65.
82. Elkanawati RY, Sumiwi SA, Levita J. Impact of lipids on insulin resistance: insights from human and animal studies. *Drug Des Devel Ther*. 2024;18:3337–60.
83. Reaven G. The metabolic syndrome or the insulin resistance syndrome? Different names, different concepts, and different goals. *Endocrinol Metab Clin North Am*. 2004;33:283–303.
84. Tucker LA. Insulin resistance and biological aging: the role of body mass, waist circumference, and inflammation. *Biomed Res Int*. 2022;2022:2146596.
85. Janssen JAMJL. Hyperinsulinemia and its pivotal role in aging, obesity, type 2 diabetes, cardiovascular disease and cancer. *Int J Mol Sci*. 2021;22:7797.
86. Kulkarni AS, Gubbi S, Barzilai N. Benefits of metformin in attenuating the hallmarks of aging. *Cell Metab*. 2020;32:15–30.
87. Fedewa MV, Gist NH, Evans EM, Dishman RK. Exercise and insulin resistance in youth: a meta-analysis. *Pediatrics*. 2014;133:e163-174.
88. Lu M, He R, Li C, Liu Z, Chen Y, Yang B, et al. Apolipoprotein E deficiency potentiates macrophage against *Staphylococcus aureus* in mice with osteomyelitis via regulating cholesterol metabolism. *Front Cell Infect Microbiol*. 2023;13:1187543.

Publisher's Note

Springer Nature remains neutral with regard to jurisdictional claims in published maps and institutional affiliations.